



## PLANT SCIENCES

# OsCYP706C2 diverts rice strigolactone biosynthesis to a noncanonical pathway branch

Changsheng Li<sup>1,2</sup>, Imran Haider<sup>1,3,4</sup>, Jian You Wang<sup>3</sup>, Pierre Quinodoz<sup>5</sup>, Hernando G. Suarez Duran<sup>6</sup>, Lucía Reyes Méndez<sup>5,7</sup>, Robin Horber<sup>5</sup>, Valentina Fiorilli<sup>8</sup>, Cristina Votta<sup>8</sup>, Luisa Lanfranco<sup>8</sup>, Samara M. Correia de Lemos<sup>6,9</sup>, Lucile Jouffroy<sup>10</sup>, Baptiste Moegle<sup>10</sup>, Laurence Miesch<sup>10</sup>, Alain De Mesmaeker<sup>5</sup>, Marnix H. Medema<sup>6,11</sup>, Salim Al-Babili<sup>3</sup>, Lemeng Dong<sup>1\*</sup>, Harro J. Bouwmeester<sup>1\*</sup>

Strigolactones exhibit dual functionality as regulators of plant architecture and signaling molecules in the rhizosphere. The important model crop rice exudes a blend of different strigolactones from its roots. Here, we identify the inaugural noncanonical strigolactone, 4-oxo-methyl carlactonoate (4-oxo-MeCLA), in rice root exudate. Comprehensive, cross-species coexpression analysis allowed us to identify a cytochrome P450, OsCYP706C2, and two methyl transferases as candidate enzymes for this noncanonical rice strigolactone biosynthetic pathway. Heterologous expression in yeast and *Nicotiana benthamiana* indeed demonstrated the role of these enzymes in the biosynthesis of 4-oxo-MeCLA, which, expectedly, is derived from carlactone as substrate. The *oscyp706c2* mutants do not exhibit a tillering phenotype but do have delayed mycorrhizal colonization and altered root phenotype. This work sheds light onto the intricate complexity of strigolactone biosynthesis in rice and delineates its role in symbiosis and development.

## INTRODUCTION

Strigolactones (SLs) are exuded by plant roots into the rhizosphere, where they function as signaling molecules inducing hyphal branching in arbuscular mycorrhizal (AM) fungi, an essential presymbiotic process. SLs also have a hormonal function in planta, regulating root architecture, shoot branching/tillering, and leaf senescence (1–4). Root parasitic plants, such as *Striga hermonthica*, have hijacked the SLs in the rhizosphere as a germination stimulant, ensuring germination in the presence of a host (5, 6). To date, more than 35 different SLs have been identified in a variety of plant species (7, 8). The SLs are generally divided into two overall categories, the canonical and the noncanonical SLs. The former can be subdivided into orobanchol- and strigol-type SLs based on the orientation of the C-ring ( $\alpha$  or  $\beta$ ) (6, 9). Unlike the relatively similar canonical SLs (all having the ABCD-ring structure), noncanonical SLs display a large structural diversity and share only the conserved D-ring (10–15).

All currently known natural SLs are derived from all-*trans*- $\beta$ -carotene (7, 16). Three enzymes—all-*trans*-9-*cis*- $\beta$ -carotene isomerase

DWARF27 (D27), carotenoid cleavage dioxygenases 7 (CCD7), and CCD8—are responsible for converting all-*trans*- $\beta$ -carotene to carlactone, the simplest SL and also the precursor of all natural SLs (17). Cytochrome P450s, belonging to family CYP711 and also known as MAX1s, exhibit diverse enzymatic function in producing various SLs from carlactone (18–21). For instance, rice MAX1 (Os900) and the *Selaginella* SmMAX1a/b convert carlactone to 4-deoxyorobanchol (4DO) (20), while another rice MAX1 (Os1400) produces orobanchol from 4DO (19, 20). The conversion of carlactone to carlactonoic acid (CLA) appears to be the most common reaction catalyzed by MAX1s and was found in *Arabidopsis*, tomato, poplar, and maize (18, 20, 21). CLA can be converted to methylCLA (MeCLA) by a CLA methyltransferase (CLAMT) (22).

In addition to MAX1, other cytochrome P450s are involved in SL biosynthesis (8). In tomato and cowpea, CYP722C catalyzes orobanchol biosynthesis from CLA, while in *Lotus japonicus* and cotton, CYP722C catalyzes 5-deoxystrigol (5DS) production, also from CLA (23–25). In sorghum, SbCYP728B35 was identified as a sorgomol synthase (26), and CYP712G1 in tomato was shown to catalyze the double oxidation of orobanchol, resulting in the formation of three didehydro-orobanchol isomers (27). In maize, ZmCYP706C37 catalyzes multiple steps in the biosynthesis of a range of SLs (28).

So far, in rice, only canonical SLs, 4DO and orobanchol, have been identified, and their biosynthesis involves two MAX1s (19). In addition, structurally unknown SLs with mass/charge ratio ( $m/z$ ) 361, coined methoxy-5DS isomers, have been reported (9, 29, 30), but nothing is known about their structures, biosynthesis, or functions in rice (29–31).

In the present study, using cross-species coexpression analysis on gene expression datasets from *Arabidopsis*, tomato, and rice, we identify a set of candidate genes for SL biosynthesis in rice. Heterologous expression of one of these candidates, OsCYP706C2, in yeast and pathway reconstruction in *Nicotiana benthamiana* allowed us to elucidate the biosynthesis of a new rice SL, 4-oxo-methyl carlactonoate (4-oxo-MeCLA), the structure of which was confirmed

<sup>1</sup>Plant Hormone Biology Group, Swammerdam Institute for Life Sciences, University of Amsterdam, Science Park 904, 1098 XH Amsterdam, Netherlands. <sup>2</sup>Yuelushan Laboratory, Hunan Provincial Key Laboratory of Plant Functional Genomics and Developmental Regulation, College of Biology, Hunan University, 410082, Changsha, P. R. China. <sup>3</sup>Division of Biological and Environmental Sciences and Engineering, King Abdullah University of Science and Technology, The BioActives Lab, Thuwal, 23955-6900, Saudi Arabia. <sup>4</sup>Department of Soil, Plant and Food Sciences, Section of Plant Genetics and Breeding, University of Bari Aldo Moro, 70121 Bari, Italy. <sup>5</sup>Syngenta Crop Protection AG, Schaffhauserstrasse 101, CH-4332 Stein, Switzerland. <sup>6</sup>Bioinformatics Group, Wageningen University & Research, 6708 PB Wageningen, Netherlands. <sup>7</sup>Department of Chemistry, University of Basel, St. Johannis-Ring 19, 4056 Basel, Switzerland. <sup>8</sup>Department of Life Sciences and Systems Biology, University of Turin, Viale P.A. Mattioli 25, 10125 Turin, Italy. <sup>9</sup>Plant genomics and transcriptomics group, Institute of Biosciences, Sao Paulo State University, 13506-900 Rio Claro, Brazil. <sup>10</sup>Equipe Synthèse Organique et Phytochimie, Institut de Chimie du CNRS UMR 7177, Université de Strasbourg, Strasbourg, France. <sup>11</sup>Institute of Biology, Leiden University, Sylviusweg 72, 2333 BE, Leiden, Netherlands.

\*Corresponding author. Email: h.j.bouwmeester@uva.nl (H.J.B.); l.dong2@uva.nl (L.D.)

by synthesis. We show that OsCYP706C2, in combination with Os900 and another previously unidentified enzyme, 4-oxo-CLA methyl transferase (Os4OCLAMT), catalyzes the formation of 4-oxo-MeCLA from carlactone. Analysis of CRISPR-Cas9 mutant lines confirmed that the *oscyp706c2* mutant is deficient in the production of 4-oxo-MeCLA. The mutant did not display a tillering phenotype, but root architecture and colonization by AM fungi were affected, suggesting a role for this rice SL in root development and AM symbiosis establishment.

## RESULTS

### Cross-species coexpression analysis reveals candidate genes for rice strigolactone biosynthesis

To identify gene candidates in SL biosynthesis, we used cross-species gene coexpression analysis, reasoning that conserved enzyme-encoding genes involved in strigolactone biosynthesis across different plant species would likely retain strong coexpression signals across evolutionary time. Hereto, publicly available transcriptome datasets from *Arabidopsis*, tomato, and rice—grown under phosphorus (P) deficiency—were used (32–34). Orthologous communities (OCs) containing genes that are coexpressed with *CCD8* were extracted (see Materials and Methods) (table S1). Four sets of genes coexpressed with *CCD8* were identified (tables S2 to S5): 151 in tomato and rice, 56 in tomato and *Arabidopsis*, 43 in *Arabidopsis* and rice, and 7 that were coexpressed with the *CCD8*s of all three species. Among the largest group are, for example, not only rice and tomato *CCD7*, demonstrating the validity of our approach, but also other noteworthy genes (highlighted in blue in table S2). Many of them are functionally annotated as involved in isoprenoid and phytohormone metabolism, symbiosis, phosphate (Pi) homeostasis, immune or defense response, and fatty acid metabolism. For instance, genes encoding  $\zeta$ -carotene desaturase (ZDS) (Solyc01g097810/ LOC\_Os07g10490), prolycopenone isomerase CRTISO (Solyc10g081650/ LOC\_Os11g36440), geranylgeranyl pyrophosphate synthase (AT2G18640/LOC\_Os07g39270), involved in the biosynthesis of the carotenoid substrate of SLs, showed coexpression with *CCD8* (tables S2 and S4). *Ent*-copalyl diphosphate synthase (Solyc06g084240/ LOC\_Os02g17780) and *ent*-kaurene oxidase (Solyc04g083160/ LOC\_Os06g37364) that encode two enzymes in the gibberellin biosynthesis pathway (35–38) also coexpressed with *CCD8*, suggesting cross-talk between SLs and gibberellin. In addition, there are genes related to Pi uptake, Pi transport, symbiosis, and immune/defense responses (tables S2 to S4) coexpressed with *CCD8*, supporting the involvement of SLs in these processes (39–41).

Of the seven genes coexpressed with *CCD8* in all three species (Fig. 1A and table S5), three belong to a gene family encoding U-box proteins (AT5G51270, LOC\_Os06g04880, and Solyc05g051610), while the others encode CYP706s (AT4G22690, Solyc08g079300, LOC\_Os01g50490, and LOC\_Os08g43440). Recently, CYP706C37 in maize was shown to be involved in zealactone biosynthesis (28), making these CYP706 genes interesting candidates to pursue further.

To obtain further insight into the two CYP706 candidates in rice, additional, publicly available, RNA sequencing (RNA-seq) data from rice roots (42) were mined by mutual rank (MR) analysis (43). Hereto, first coexpression relationships between the known rice SL biosynthetic genes (*OsCCD7*, *OsCCD8*, *Os900*, and *Os1400*; *OsD27* was not found in the dataset) were calculated (Fig. 1A). The expression of three of these genes—*OsCCD7*, *OsCCD8*, and *Os900*—showed the strongest correlation, while *Os1400* expression

was less similar. The former three tightly coexpressed genes were then used as baits to identify additional genes with a similar expression profile (Fig. 1B). Among the top 5 ranked candidates was also one CYP706, *LOC\_Os01g50490/OsCYP706C2* (highlighted in Fig. 1C) (44).

Intriguingly, this *OsCYP706C2* gene, but not the other CYP706/LOC\_Os08g43440, is located close to the two known rice SL biosynthetic genes (*Os900* and *Os1400*) on chromosome 1 (Fig. 1D, fig. S1A, and table S6). Among the six annotated genes in this region (~73 kb), we also noticed another candidate gene, *LOC\_Os01g50480* (annotated as encoding a putative SAM-dependent carboxyl methyltransferase), which also had a relatively high ranking in our coexpression analysis (Fig. 1C). In addition to this gene, a close homolog (*LOC\_Os01g50610*) sharing high sequence similarity is also located in the same region, suggesting the presence of a biosynthetic gene cluster (BGC). Both methyltransferase genes are homologs of *Arabidopsis CLAMT* that was recently shown to be involved in the biosynthesis of MeCLA (22, 45). To gain further insight into the candidate genes from this genomic region, we looked at their expression in roots, including in plants exposed to different Pi treatments (42, 46). Expression of most of these genes is induced when plants are exposed to Pi deficiency and down-regulated when Pi is resupplied, a pattern typical of SL genes as well as in other plant species (32, 33, 42). *OsCYP706C2* and *Os900* display a highly similar expression profile, while the two methyl transferase genes are less coexpressed (fig. S1, B and C).

To further investigate the origin of this apparent BGC, we performed gene cluster analysis across the phylogenetic tree of CYP706s (Fig. 1D, figs. S2 and S3, and table S7). In most plant species, *CYP711s* are absent from the region neighboring *CYP706*, whereas methyltransferases do generally cluster there. However, a notable exception is a BGC that contains all three types of genes (*CYP706*, *CYP711*, and the methyltransferase) that is present only in Poaceae. The maize BGC, for example, has three genes (*ZmCYP706C37*, *ZmMAX1b*, and *ZmCLAMT1*), and these are indeed involved in maize SL biosynthesis (28). In different rice species, different combinations of (duplicates of) these genes occur, and switchgrass—*Panicum virgatum* that also contains this BGC—displays even more variation and duplication (Fig. 1D and fig. S2). Together, these findings led us to postulate that the other uncharacterized genes in the rice BGC from *Oryza sativa* ssp. *indica* and *O. sativa* ssp. *japonica* (fig. S2) likely encode SL biosynthetic pathway enzymes. These genes are *OsCYP706C2* and two putative methyl transferases, *LOC\_Os01g50480* and *LOC\_Os01g50610*.

### Identification of 4-oxo-MeCLA, a natural rice strigolactone

Considering the similarities to the maize SL biosynthesis pathway (28), we hypothesized that the unknown rice SL, with a mass  $[M + H]^+$  of 361 (9, 29, 30), could be 3-oxo-MeCLA, an intermediate in the conversion of MeCLA to zealactone and also itself a SL in the root exudate of maize (28). The retention time of 3-oxo-MeCLA, however, was different from this unknown rice SL, so we assumed that it must be an isomer, possibly 4-oxo-MeCLA. A standard for unequivocal identification of 4-oxo-MeCLA was synthesized by Stille cross-coupling and adapting the versatile approach previously developed by Dieckmann *et al.* (47) for noncanonical SLs (fig. S4A). A thorough analysis with  $^1\text{H}$  and  $^{13}\text{C}$  nuclear magnetic resonance (NMR) unambiguously confirmed the identity of the synthetic sample obtained (fig. S5). The 4-oxo-MeCLA displays enhanced

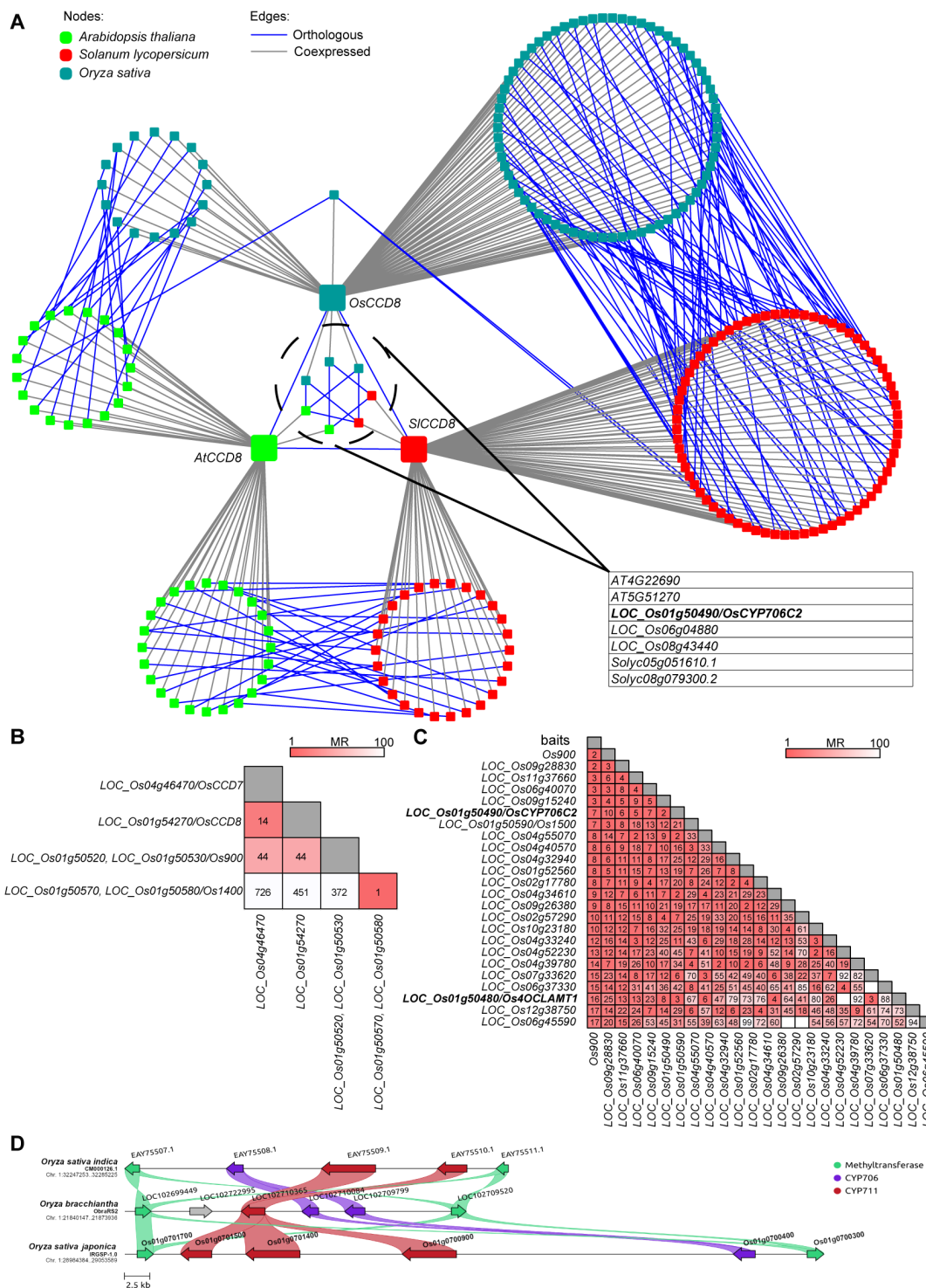


**Fig. 1. Screening for rice strigolactone biosynthetic genes.** (A) Cross-species coexpression network of the CCD8 OCs. Nodes represent genes, colored by species: *A. thaliana* genes are green, *Solanum lycopersicum* genes are red, and *O. sativa* genes are teal. The large nodes represent the bait genes (CCD8). Gray edges link genes that are coexpressed (Pearson’s correlation coefficient > 0.7), and blue edges link orthologous genes. (B) Heatmap showing the correlation of four rice strigolactone (SL) biosynthetic genes. Mutual rank analysis of four rice SL biosynthetic genes. (C) Heatmap depicting the top 24 genes coexpressed with three tightly coexpressed rice SL genes (*OsCCD7*, *OsCCD8*, and *Os900*). The three genes combined were used as the “reference compound gene” (“sum” method). Low numbers in squares indicate supportive MR scores (<100). Panels (B) and (C) are based on mutual rank (MR) analysis using published root RNA-seq data (see Materials and Methods). Candidate genes that are functionally characterized are highlighted in bold. (D) Putative SL BGC from three *Oryza* species. Genome assembly name/version or NCBI accession, chromosome, and chromosomal coordinates in base pair are indicated for each species. The three families of SL biosynthetic genes are presented in green, purple, and red, while one “intervening” gene that resides in between is shown in gray.

chemical stability compared with MeCLA, likely due to the extra carbonyl removing electron density from the triene moiety. This increased stability probably facilitates the detection of 4-oxo-MeCLA in root exudates. Using this standard, an Multiple Reaction Monitoring (MRM) method was developed (Fig. 2A and fig. S4B) and used to demonstrate that 4-oxo-MeCLA is indeed present in the root exudate of wild-type (WT) Nipponbare rice (Fig. 2B).

### Functional characterization of *OsCYP706C2*

Initially, we considered it likely that *in vivo* production of 4-oxo-MeCLA would proceed from MeCLA, possibly through the catalytic activity

of *OsCYP706C2*. We thus used MeCLA as the substrate in an assay with yeast microsomes expressing *OsCYP706C2*. After 1 hour, no significant difference was observed between microsomes expressing *OsCYP706C2* and the control (fig. S6A). After a 3-hour incubation, microsomes expressing *OsCYP706C2* produced a bit more 4-oxo-MeCLA than the control, although most of the supplied MeCLA substrate remained (fig. S6B). Transient expression of the MeCLA pathway (using maize genes) in combination with *OsCYP706C2* in *N. benthamiana* resulted in a reduction in MeCLA levels and the production of some 4-oxo-MeCLA. However, the abundance of the latter did not differ significantly from that in the control

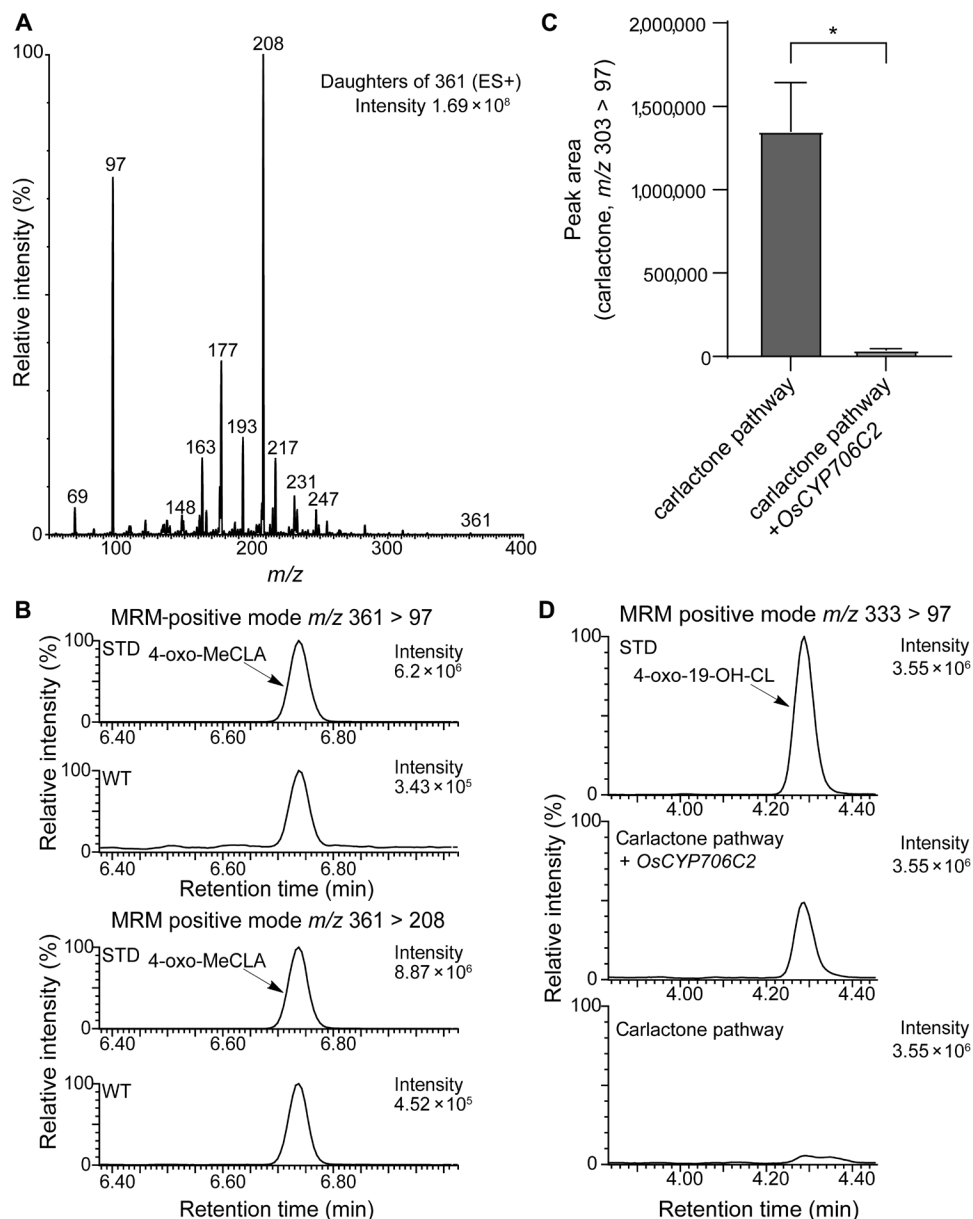


**Fig. 2. Discovery of one new non-canonical rice strigolactone (4-oxo-methyl carlactonoate) and functional characterization of *OsCYP706C2*.** (A) MS-MS fragmentation spectra of the synthetic 4-oxo-MeCLA standard. (B) Confirmation of 4-oxo-MeCLA (transition  $[M + H]^+$   $m/z$  361 > 97) in root exudates from rice wild type (WT) using the synthetic standard (STD). (C) Quantification of carlactone agroinfiltrated *N. benthamiana* leaf samples. “Carlactone pathway” includes three genes (*D27*, *CCD7*, and *CCD8*). Bars represent means  $\pm$  SEM. ns, not significant; \* $P$  < 0.05, \*\* $P$  < 0.01, and \*\*\* $P$  < 0.001 (two-tailed, unpaired *t* test). (D) Representative MRM-LC/MS/MS chromatograms of 4-oxo-19-OH-carlactone (transition  $[M + H]^+$   $m/z$  333 > 97) in *N. benthamiana* leaf samples transiently expressing carlactone pathway genes and *OsCYP706C2*.



(fig. S6, C and D). In addition, even without *OsCYP706C2*, the expression of just the maize MeCLA pathway resulted in the production of a trace amount of 4-oxo-MeCLA, which might have been formed nonenzymatically or through a *N. benthamiana* enzyme. All the above results suggest that MeCLA is not the substrate for ZmCYP706C2.

Considering that the maize homolog of *OsCYP706C2*, ZmCYP706C37, can catalyze the production of zealactol from carlactone (28), we decided to test carlactone as substrate for *OsCYP706C2*. Transient expression in *N. benthamiana* showed that, indeed, upon the expression of *OsCYP706C2* with the carlactone pathway, almost all of the carlactone was used (Fig. 2C). This probably also explains the decrease in MeCLA production in the *N. benthamiana* agroinfiltration assay, described above, as its precursor carlactone was consumed by *OsCYP706C2*.

Previous research showed that an SL “CL + 30” highly accumulated in the root exudate of *os900* mutants (48, 49). We considered that this is a product from the conversion of CL catalyzed by *OsCYP706C2* and maybe an intermediate en route to 4-oxo-MeCLA. To verify this hypothesis, we synthesized 4-oxo-19-OH-carlactone as a candidate structure for CL + 30 (fig. S7). This primary alcohol was obtained by applying the same strategy developed to synthesize zealactol (28). The structure was unambiguously confirmed by NMR analysis, and the compound was stable at  $-18^{\circ}\text{C}$  in a dichloromethane solution (1 mg/ml) (fig. S8). Using this standard, an MRM method was developed and used to analyze samples of *N. benthamiana*, in which we transiently expressed the carlactone pathway with and without *OsCYP706C2* (Fig. 2D and fig. S7). Abundant 4-oxo-19-OH-carlactone accumulated when *OsCYP706C2* was expressed together with the carlactone pathway genes (Fig. 2D), demonstrating the conversion by *OsCYP706C2* of carlactone to 4-oxo-19-OH-carlactone as intermediate en route to 4-oxo-MeCLA.

### Elucidation of 4-oxo-MeCLA biosynthesis

We subsequently postulated that, analogous to zealactone biosynthesis in maize, one of the rice MAX1s and a methyl transferase are required for biosynthesis of 4-oxo-MeCLA from 4-oxo-19-OH-carlactone (Fig. 3A). As indicated above, previous research (48, 49) suggests that *Os900* is the most likely candidate for this conversion because 4-oxo-19-OH-carlactone (CL + 30) accumulated in *os900* mutant root exudate. In addition, our MR analysis showed that *Os900* ranks highly in the list of coexpressed genes with *OsCYP706C2* (fig. S1D). Transient expression of *OsCYP706C2* and *Os900* together with the rice carlactone pathway genes (*OsD27*, *OsCCD7*, and *OsCCD8*) resulted in the formation of a further oxidized product, detected using parent iron scanning, which we believe to be 4-oxo-carlactonoic acid (Fig. 3B). Addition to the latter gene combination of each of the two methyl transferase candidates (*LOC\_Os01g50480* and *LOC\_Os01g50610*) resulted in production of 4-oxo-MeCLA (Fig. 3B). As a result, we named these two methyltransferases *Os4OCLAMT1* and *Os4OCLAMT2* (*O. sativa* 4-oxo carlactonoic acid methyl transferases 1 and 2).

As reported, *Os900* and *Os1400* catalyze canonical SL biosynthesis (4DO and orobanchol) in rice (19). Therefore, we designed an agroinfiltration experiment using different combinations of these genes, aiming to reconstitute the complete rice SL biosynthetic pathway (Fig. 3D and fig. S9, A to D). The large production of 4DO was achieved by combining the carlactone pathway genes with *Os900*, *OsCYP706C2*, and the two methyl transferases (fig. S9A), while combinations with *Os900* plus *Os1400* produced more orobanchol (fig. S9B). Both gene combinations also resulted in the formation of 4-oxo-MeCLA (fig. S9 C).

Together, we conclude that *OsCYP706C2* catalyzes the conversion of carlactone to 4-oxo-19-OH-carlactone, which is subsequently converted to 4-oxo-carlactonoic acid by *Os900* and then to 4-oxo-MeCLA by *Os4OCLAMT* (Fig. 3A and fig. S9D). There are two possible paths for the conversion of carlactone to 4-oxo-19-OH-carlactone by *OsCYP706C2*, which is hydroxylation first at C19 or first at C4 (fig. S9D). In maize, we demonstrated that the ortholog, ZmCYP706C37, first catalyzes the C19 hydroxylation of carlactone (28), so we assume that this is also what happens in rice.

### Mutation of *OsCYP706C2* affects root development in rice and the interaction with AM fungi

Mutant lines of *OsCYP706C2* were generated using CRISPR-Cas9 genome editing (Fig. 4A). Three T2 homozygous lines with mutations causing frameshifts were selected for further analysis. Our MRM-liquid chromatography-tandem mass spectrometry (LC-MS/MS) analysis showed that all three *oscyp706c2* mutant lines were deficient in 4-oxo-MeCLA, while orobanchol and 4DO were not affected (Fig. 4B and fig. S10). To further explore the effect of the *OsCYP706C2* mutation, rice was grown in two different culture systems (Fig. 5A). In sand, under normal Pi availability, the *oscyp706c2* mutants displayed no morphological difference and no changes in tiller number or shoot length (Fig. 5A). In hydroponics, the *oscyp706c2* mutants did also not display a tillering phenotype or dwarfism, but they had a reduced number of crown roots, especially under normal Pi, and a lower root fresh weight, especially under Pi deficiency (Fig. 5, B and C). Roots of the *oscyp706c2* mutants tended to be longer under both normal and low Pi availability while there was no consistent effect on shoot fresh weight (Fig. 5, B and C). Root exudates of the *oscyp706c2* mutant seedlings grown under low Pi contained a higher concentration of 4DO and orobanchol, suggesting divergence of SL flux into the canonical branch as a result of the mutation in the noncanonical branch (fig. S13A). Moreover, a “4-oxo-MeCLA isomer” with the same mass as 4-oxo-MeCLA was found, also with higher content in the *oscyp706c2* mutants. Further study will need to elucidate its structure and biosynthesis.

To investigate whether the change in SL profile in the *oscyp706c2* mutants affects the interaction between rice and *S. hermonthica*, we performed a *Striga* germination bioassay using the root exudate of the mutants (fig. S11). *Striga* germination in exudates from mutants and WT did not significantly differ. A *Striga* germination bioassay with the authentic standard of 4-oxo-MeCLA showed that this molecule has an activity comparable to GR24 at 0.25  $\mu\text{M}$  but did not induce germination at 2.5 nM (fig. S11). In an assay to evaluate AM symbiosis, the expression of two plant AM marker genes (*OsPt11* and *OsLysM*) (50, 51) was strongly reduced, by 50 and 80%, in two of the three mutant lines during the early stages of mycorrhization [14 days post inoculation (dpi)] (Fig. 4C). At 50 dpi, this difference had disappeared (fig. S12). The morphological data were in line with the molecular results: In the early stage of mycorrhization, the same two mutant lines displayed a significantly reduced intensity of mycorrhization (M%) and arbuscule abundance (A%) (Fig. 4D). At a later stage (50 dpi), only one mutant line still showed a decreased arbuscule abundance (fig. S12).

Together, these data show that mutation of *OsCYP706C2* hampers 4-oxo-MeCLA biosynthesis and exudation, which give rise to changes in root development, such as a decreased number of crown roots under control conditions, a decrease in root fresh weight under Pi deficiency, and a delay in AM symbiosis.

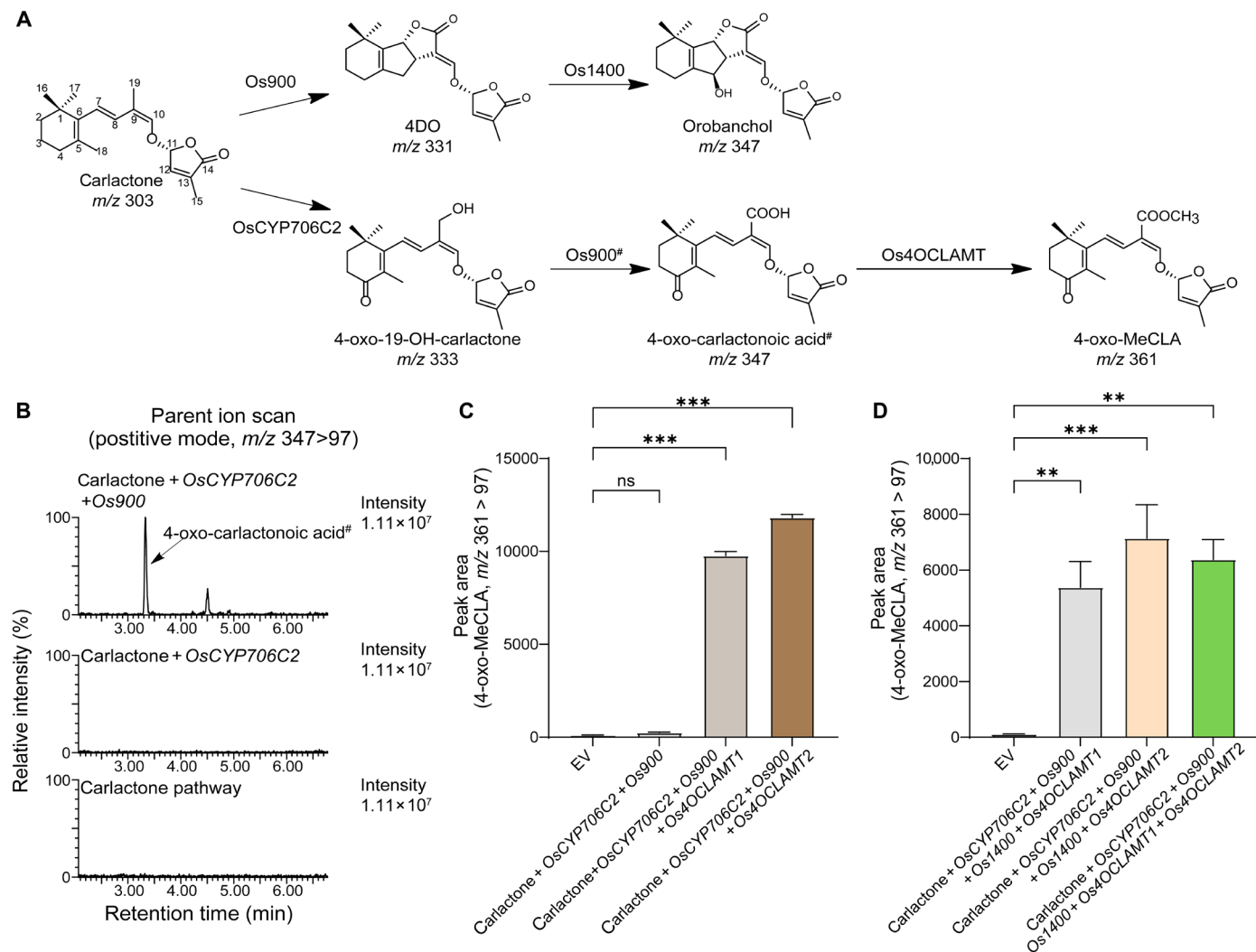


**Fig. 3. Reconstitution of rice strigolactone biosynthetic pathways in *N. benthamiana*.** (A) Scheme of biosynthesis pathways for rice SLs. The molecular weight (MW) of each compound is shown under the name. The putative steps and compound are indicated by hashtag (#). (B) Detection of putative 4-oxo-carlactonoic acid using parent ion scan (transition  $[M + H]^+ m/z$  347 > 97) in *N. benthamiana* leaf samples transiently expressing carlactone pathway genes and downstream rice SL biosynthetic genes. (C and D) Detection of 4-oxo-MeCLA (transition  $[M + H]^+ m/z$  361 > 97) in agroinfiltrated *N. benthamiana* leaf using rice SL genes. EV, empty vector control. Bars represent means  $\pm$  SEM. Significant values [by one-way analysis of variance (ANOVA)] are shown with asterisks (\*\* $P < 0.01$  and \*\*\* $P < 0.001$ ).

## DISCUSSION

In the present study, we successfully identified a previously unknown SL, 4-oxo-MeCLA, in rice root exudate and elucidated its biosynthetic pathway by characterizing two so far unknown enzymes, OsCYP706C2 and Os4OCLAMT. We thus show that rice, in addition to canonical SLs, also produces and exudes into the rhizosphere, a noncanonical SL. Previously, putative canonical “methoxy-5DS isomers” were detected in rice root exudates, but their structure and biosynthesis remained elusive (29–31). We conclude that one of these methoxy-5DS isomers is 4-oxo-MeCLA, a noncanonical SL. In addition, we show that the 4-oxo-MeCLA biosynthetic pathway of rice involves OsCYP706C2, Os4OCLAMT, and the previously identified rice MAX1 (Os900).

Initially, we thought that the first of these enzymes, OsCYP706C2, was responsible for the conversion of MeCLA to 4-oxo-MeCLA. However, OsCYP706C2 did not effectively consume MeCLA, and

therefore, we hypothesized that biosynthesis of 4-oxo-MeCLA proceeds from carlactone. We then showed that OsCYP706C2 indeed uses carlactone as a preferred substrate. Moreover, using chemical synthesis, we demonstrated that OsCYP706C2 catalyzes the formation of 4-oxo-19-OH-carlactone as intermediate en route to 4-oxo-MeCLA. The 4-oxo-19-OH-carlactone subsequently serves as substrate for Os900 and Os4OCLAMT that introduce the methoxy group. This finding implies that rice MAX1 (Os900) has an additional enzymatic activity that has not been characterized before. In maize, we demonstrated that ZmMAX1b is also involved in two parallel pathways that both lead toward biosynthesis of zealactone and other maize SLs (28). In rice, we now show that MAX1 (Os900) is also involved in two pathways, catalyzing the formation of the canonical SL, 4DO, from carlactone as reported before (19), and the conversion of 4-oxo-19-OH-carlactone to 4-oxo-carlactonoic acid. Os900 is thus important for biosynthesis of both canonical and noncanonical

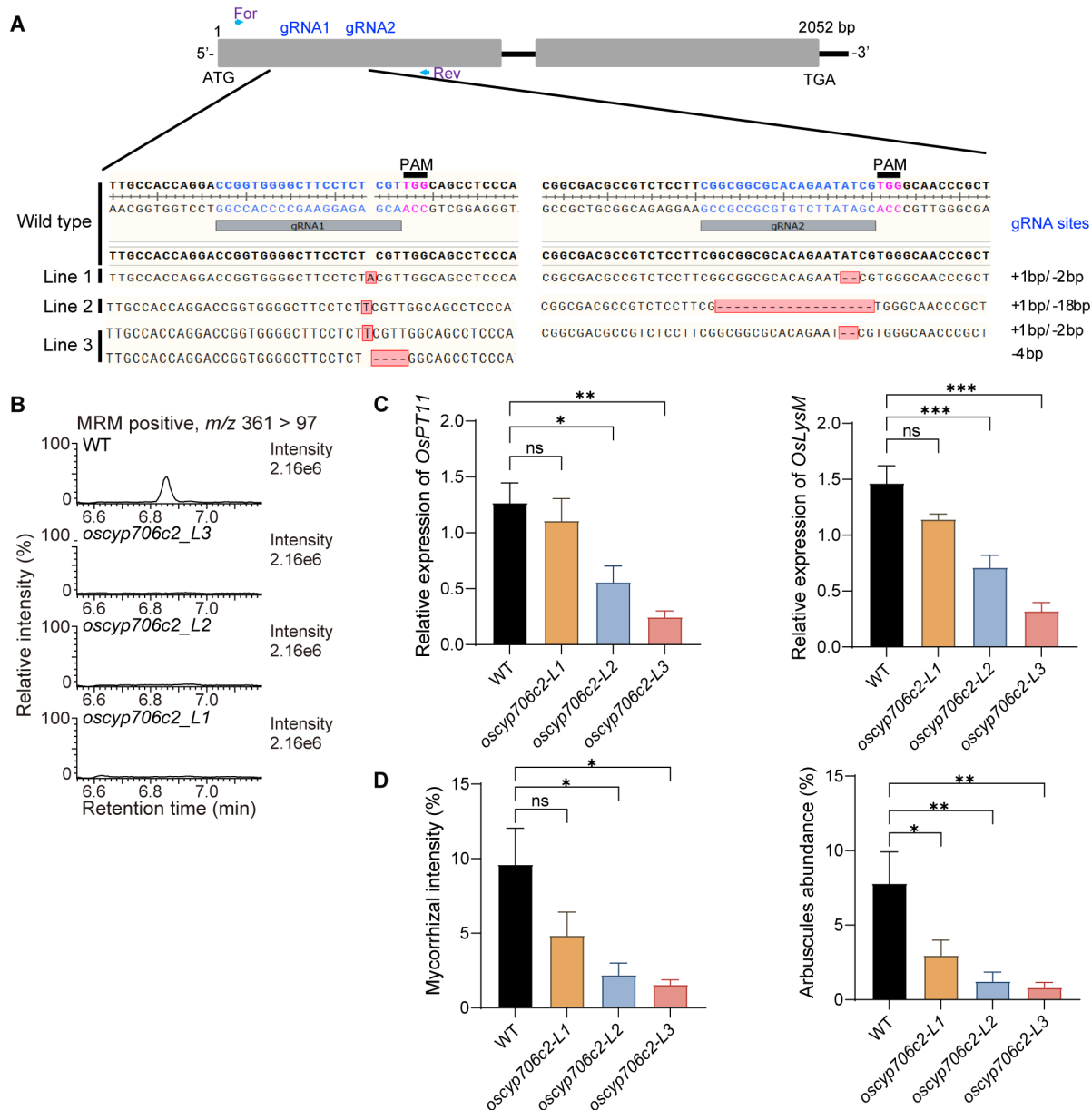


**Fig. 4. Characterization of *oscyp706c2* mutants.** (A) Generation of *oscyp706c2* mutants. The structure of *OsCYP706C2* and the two CRISPR-Cas9 target sites. Target sites are presented with blue letters, and the neighboring protospacer adjacent motifs (PAM) are also highlighted. The sequences of the targeted region for WT and mutant lines are shown. Mutation effects are indicated at the right of their corresponding sequences. (B) Representative chromatograms of detection for 4-oxo-MeCLA from root exudates of rice seedlings, showing the deficiency of 4-oxo-MeCLA in *oscyp706c2* mutants. (C) Quantitative reverse transcription polymerase chain reaction analysis of two AM-responsive marker genes (*OsPT11* and *OsLysM*) in mycorrhizal roots at early stage of development [14 days post inoculation (dpi)]. (D) Evaluation of rhizospheric interactions with AM fungus *R. irregularis* at 14 dpi. Mycorrhizal intensity (M%) and arbuscule abundance (A%) in the root system of WT and *oscyp706c2* mutants were calculated. Data are means  $\pm$  SE ( $n = 4$  biological replicates). Significant values (by one-way ANOVA) are shown with asterisks (\* $P < 0.05$ , \*\* $P < 0.01$ , and \*\*\* $P < 0.001$ ).

SLs in rice. *os900* mutants do not exude 4DO and orobanchol anymore, while “CL + 30” (which we here identify as 4-oxo-19-OH-carlactone) accumulated in the exudate (48, 49). Nevertheless, the authors still detected a trace of 4-oxo-MeCLA in the root exudate of the *os900* mutant (48, 49), suggesting the existence of a minor bypass, independent of *Os900*, possibly catalyzed by one of the other rice MAX1 homologs. The methyl transferases (*Os4OCLAMT*) that we identified in the present study catalyze the last step in the biosynthesis

of 4-oxo-MeCLA using 4-oxo-CLA as a substrate and not CLA as in *Arabidopsis* CLAMT (45). Earlier it was shown that the two rice methyl transferases can also convert CLA to MeCLA (33). Why there are two copies of this enzyme and whether they have separate functions will need further investigation in rice, as well as in a range of other species that also have two copies of this enzyme.

An increasing number of noncanonical SLs are being found in different species such as sunflower, maize, and black oat (7, 10, 11,

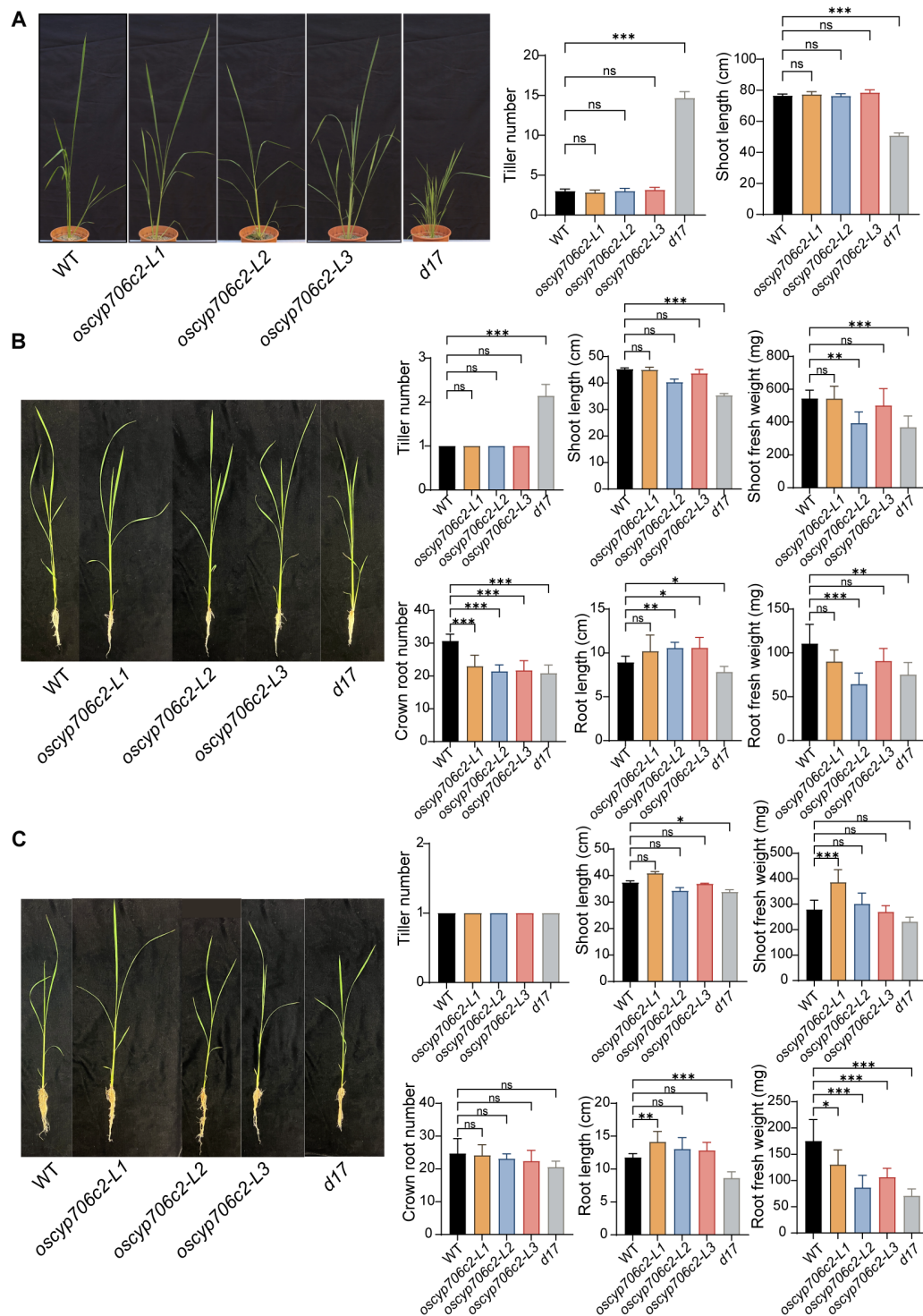


**Fig. 5. Phenotyping of *oscyp706c2* mutants.** (A) Phenotypic characterization of *oscyp706c2* mutants grown on sand. Seedling architecture, shoot length and number of tillers of Nipponbare WT, *oscyp706c2* three mutant lines, and *d17* at young stage (40-day-old seedlings) grown under +P conditions. (B and C) Phenotypic characterization of *oscyp706c2* mutants on hydroponics under normal Pi (B) and low Pi availability. (C) Seedling architecture, tiller number, shoot length, shoot fresh weight, crown root number, root length, and root fresh weight of rice lines. Data are means  $\pm$  SE ( $n = 6$  biological replicates). Significant values (by one-way ANOVA) are shown with asterisks (\* $P < 0.05$ , \*\* $P < 0.01$ , and \*\*\* $P < 0.001$ ).



13–15, 52, 53). These findings have spurred increasing interest in the role and biological significance of canonical and noncanonical SLs (15). It is still challenging to precisely quantify the concentration/content of different SLs (due to instability, matrix effects, etc.), and according to the literature, there are large differences in the relative production of SLs between different rice genotypes. For root exudates of Nipponbare, based on published results (48, 49) and our data shown here in fig. S13A, it seems that the content of 4-oxo-MeCLA and 4DO is higher than that of orobanchol, at least under the conditions we used. In this study, we show that the *oscyp706c2* mutants, which lack the noncanonical 4-oxo-MeCLA, display delayed colonization by AM fungi compared with the WT. This suggests that 4-oxo-MeCLA is involved in the early stages of AM symbiosis establishment. Although there is no report of an effect of noncanonical SLs on mycorrhizal colonization, noncanonical SLs were shown to induce hyphal branching in AM fungi (54, 55).

In contrast, no difference was observed in the induction of *Striga* germination between root exudates from *oscyp706c2* mutant and control plants. The mutants still produced 4DO and orobanchol, both known stimulants of *Striga* germination (56, 57). The synthetic 4-oxo-MeCLA did induce *Striga* germination, but with much lower activity than for example orobanchol (57).

The *oscyp706c2* mutants did not display an increased tillering or dwarfism phenotype, whereas dysfunction of SL genes encoding upstream steps in SL biosynthesis, such as for example in mutant *d17*, results in more tillering and dwarfing (Fig. 5A). *Os900* knockout mutants also did not display a shoot phenotype, in contrast to mutations in *Os1900* and *Os5100* that in vitro catalyze the CL to CLA conversion (48, 58). This suggests that upstream SLs (such as CL and CLA) are precursor of the SL hormone regulating tillering and thus play a critical role in the regulation of rice shoot architecture, while downstream SLs such as 4DO, orobanchol, and 4-oxo-MeCLA—that are exuded from the roots—do not. However, we do observe a root development phenotype in the *oscyp706c2* mutants (Fig. 5, B and C), indicating a role for *OsCYP706C2* in the biosynthesis of a hormonal, noncanonical strigolactone-like molecule that is involved in the regulation of root development. Supporting this is the observation that growth of nodal roots in *zmccd8* maize seedlings was delayed (59).

Our analysis of the putative BGC and its phylogeny showed that it is conserved among other grass species (Fig. 1D and fig. S2). In switchgrass (*P. virgatum*), for example, the putative SL BGC contains three copies of *CYP706*, two of *CYP711/MAX1*, and two methyltransferases. Switchgrass root extracts and exudates induce germination of *Orobanche cumana* seeds (60). In the wild rice relative, *Oryza brachyantha* (61), the SL BGC contains one *CYP711/MAX1*, two *CYP706s*, and two methyltransferases. All this suggests the presence of SLs in these species, likely noncanonical, but so far there is no information about the identity of the SLs they produce. The identification of these BGCs may help in the identification of the SLs of these and other so far unexplored species. Using a BLAST search on National Center for Biotechnology Information (NCBI), we identified 163 *CYP706* homologs across 46 plant species (partially shown in figs. S2 and S3 and table S7). These *CYP706* genes are distributed from the Amborellaceae to the Cupressaceae (gymnosperms) and include three families in the monocots and two major clades in the dicots. In the monocots, two *CYP706* genes appear in the families Orchidaceae and Dioscoreaceae (figs. S2 and S3). In the Poaceae, 17 *CYP706* genes are distributed across two clades. One of the clades includes *ZmCYP706C37* (XP\_008673660.1) that is located in the

BGC for SL biosynthesis in maize, whereas the second clade includes no known SL genes (figs. S2 and S3 and table S7). In dicots, *CYP706* genes are present in 19 families. In the Rosaceae, 13 *CYP706* genes are distributed among three species, *Malus domestica*, *Fragaria vesca*, and *Rosa chinensis*, whereas the distribution across other species is scattered. More functional investigation is needed to further our understanding of the function of all these *CYP706s* in plants.

In conclusion, we identified a natural noncanonical SL, 4-oxo-MeCLA, in rice and elucidated its biosynthetic pathway and functions in root development and symbiosis with AM fungi. Others have already shown that the SLs in rice root exudate affect the composition and functions of the root-associated microbiome and AM symbiosis (48, 49, 62). However, more investigations will be needed to pinpoint the exact rhizosphere signaling roles of all these structurally different rice SLs and how they differ between cultivars/varieties and species and under different (nutrient) stress conditions. Although we now know which genes/enzymes are involved in the biosynthesis of almost all rice SLs, there are still other unknown SLs remaining in rice, the other two putative “methoxy-5DS isomers” reported in earlier work (9, 29–31). As we noticed here, there is a 4-oxo-MeCLA isomer that increased in concentration in the *oscyp706c2* mutants, which likely represents one of the other “methoxy-5DS isomers.” Further work should shed light on the biosynthesis and functions of these last unknown rice SLs.

## MATERIALS AND METHODS

### OCs analysis

The RNA-seq data were obtained from published resources (32, 33) or retrieved from NCBI’s Gene Expression Omnibus (with identifier GSE74856) (34). Expression analysis for OCs was performed in R 3.6.1 with the edgeR package 3.26.8 (63). Genes with less than one count per million reads mapped in at least two samples were removed. Reads were normalized by library and exon size (reads per kilobase per million mapped reads). Coexpression (for OCs analysis) was defined for each plant species and tissue independently using Pearson’s correlation coefficient (PCC). Gene pairs with PCC < 0.7 were removed. The results were used to create transcriptome network per plant species, with genes represented as nodes and edges representing coexpressed gene pairs. The networks were then integrated with edges linking genes with known orthologous relationships, as retrieved from EnsemblPlants (Release 39) (64) through the BioMart data mining tool (65). The OC of the target gene *CCD8* (*At4g32810*, *Solyc08g66650*, and *Os01g0746400/LOC\_Os01g54270*) is a cross-species coexpression network defined by the group of genes that are coexpressed with *CCD8* in more than one species, as identified through orthologous relationships. OCs are generated by: (i) isolating the coexpression neighborhood of *CCD8*, (ii) identifying the target’s ortholog in another species and isolating the corresponding neighborhood, and (iii) removing genes that have orthologs not coexpressed with *CCD8*. The code for the computational workflow to identify OCs and orthologous differentially expressed communities from cross-species transcriptome data can be found online at <https://bitbucket.org/her191/cade-heron/>.

### Coexpression and transcript expression analysis

MR-based global gene coexpression analysis was performed using RStudio (R version 3.4.0) (43, 66). The transcript data were

obtained from Rice Expression Database (<https://ngdc.cnpc.ac.cn/red/index>) (46).

### Gene cluster and phylogeny analysis

Gene cluster analysis was performed using cblaster v.1.3.6 (67), and a gap parameter of 200 kb and setting methyltransferase sequences as required were set. After filtration and exclusion of overlapping sequences, the resultant sequences were then grouped into homologs for methyltransferases, CYP711s and CYP706s. The HMMER profiles files were obtained from the Pfam library (68). Two profiles (PF00067.24 for cytochrome P450 and PF03492.17 for SAM-dependent carboxyl methyltransferase) and hmmlign/ HMMER v.3.3 (69) were used for of candidate sequences alignment.

Online NCBI BLASTp server (70) was used identify CYP706 homologues (amino acid identity threshold  $\geq 40\%$ ). For CYP706 candidates, cytochrome P450 domains were extracted using a protocol from <https://github.com/alevchuk/finding-the-sequence-of-a-domain>. The output was aligned using wrapper from Galaxy version 13.45.0.4846264 (71), generating a multiple sequence alignment (MSA) with a score of 970. We retrieved two protein sequences CYP81D of *Arabidopsis thaliana* from the cytochrome p450 homepage (72) to use as an outgroup on the MSA. The MSA result was trimmed with trimAL v1.2.rev59 (73) with the automated parameter. The trimmed MSA was then used to build a phylogenetic tree with RAxML v.8.2.12 (74) with best model auto selection for proteins. The tree layout was depicted using the online tool iTOL (<https://itol.embl.de/>).

### Vector construction for generation of *OsCYP706C2* knockout plants

We used CRISPR-Cas9 technique in rice *O. sativa* L. ssp. *japonica* cv. Nipponbare for targeting *OsCYP706C2* gene (LOC\_Os01g50490). *OsCYP706C2* was targeted at two different sites, included in an exon region, and two guide RNAs (gRNAs) were designed by using the CRISPR-PLANT database (<http://omap.org/crispr/>). *OsCYP706C2* genomic sequence was targeted from 97 to 116 base pairs (bp) by gRNA-1 (5'- CCGGTGGGGCTTCCTCTCGTTGG-3') and from 321 to 340 bp by gRNA-2 (5'- CGGCGGCGCACAGAAATC-GTGG-3'); the underlined represents the PAM sequence. The construction of the transfer RNA-gRNACas9 cassette was done through Golden Gate assembly into pRGEB32 binary vector. The gRNA cassette was under the control of the rice U3 snoRNA promoter (*OsU3*), while the expression of Cas9 gene is regulated by the rice ubiquitin promoter (*OsUBI*) (75). The pRGEB32 construct was further introduced into Nipponbare wild-type *japonica* rice cultivar by *Agrobacterium tumefaciens* (strain *EHA105*)-mediated transformation as previously described (76).

### Rice transformation and mutant screening

Rice transformation was performed as previously described (76). Briefly, rice calli induced from Nipponbare mature seeds were transformed with *Agrobacterium*, and the resulting callus were grown, selected, and regenerated in presence of Hygromycin antibiotic. Once the shoots emerged, root development was promoted. All the previous steps were performed on a Percival growth chamber (CLF Plant Climatics GmbH, model CU 36L5). Regenerated plants were transferred to soil and grown in a greenhouse at 28°C day/22°C night.

The insertion of the plasmid in the transgenic plants was confirmed by polymerase chain reaction (PCR) (Taq DNA Polymerase,

Thermo Fisher Scientific) with pRGEB32-specific primers (table S8). For detection of CRISPR-mediated mutations, the targeted sequence was PCR-amplified (Phusion DNA Polymerase, NEB) with the genome specific primers (table S8). The resulting 660-bp-long PCR product was purified and cloned using the CloneJET PCR Cloning Kit (K1232, Thermo Fisher Scientific). Insertion-deletions mutations (Indels) on target site were detected by Sanger sequencing, and up to 10 colonies were analyzed. T2 homozygous lines were further examined.

### Sand and hydroponic culture of rice seedlings

Nipponbare WT, three mutant lines of *oscyp706c2*, and *d17* (positive control, more tillers than WT) were grown in river sand (1.5-liter pot) under +Pi conditions. Shoot length and tiller numbers were quantified 40 days after sowing.

The mutants were also phenotyped in hydroponics on a half-strength modified Hoagland nutrient solution with sufficient Pi (0.4 mM  $K_2HPO_3 \cdot 3H_2O$ ) and with low Pi (0.004 mM  $K_2HPO_3 \cdot 3H_2O$ ), essentially as described previously (48). The solutions were refreshed every 3 days. A number of growth and development parameters (root length, shoot length, etc.) were quantified 3 weeks after sowing.

### Chemical synthesis and structure confirmation

All chemicals and reagents used were obtained commercially. Chromatography and recording of NMR spectra were carried out as described before (47, 77). The synthesis of compounds W, Y, and Z has been previously reported in the literature, and they were obtained by reproducing the described procedures (28, 47, 78).

#### Synthesis of compound X

Compound W (374 mg) was dissolved in dichloromethane (15 ml). To the solution was added  $K_2CO_3$  (5.0 equiv.) followed by a portion-wise addition of Dess-Martin periodinane (3.0 equiv.). The resulting mixture was stirred for 2 hours at room temperature and quenched with  $Na_2S_2O_3$  10% (5 ml) at 0°C. The organic phase was washed twice with a saturated aqueous solution of  $NaHCO_3$  (2 × 10 ml), dried over  $Na_2SO_4$ , and concentrated under vacuum. The reaction product was purified using silica column chromatography (eluted with CyH/EtOAc 95/5) to give a colorless oil, compound X (260 mg, 70%).

#### Synthesis of 4-oxo-MeCLA

Compound Y (75 mg) was added to a solution of compound X (2.0 equiv.) and triphenylarsine (0.4 equiv.) in dioxane (2.3 ml). The mixture was degassed by argon bubbling for 5 min, and  $Pd_2dba_3$  (0.10 equiv.) was added. This was stirred at 80°C for 30 min, cooled down to room temperature, and filtered over celite (eluted with EtOAc), and any volatiles were removed under vacuum. The product was purified using silica column chromatography (eluted with CyH/EtOAc, gradient 100:0 to 40:60) to give 4-oxo-MeCLA as a pale yellow oil (40 mg).

#### Synthesis of 4-oxo-19-OH-carlactone

Compound Z (15 mg) was added to a solution of compound X (2.0 equiv.) and triphenylarsine (0.4 equiv.) in dioxane (0.7 ml). The mixture was degassed by argon bubbling for 5 min, and  $Pd_2dba_3$  (0.10 equiv.) was added. This was then stirred at 80°C for 30 min, cooled down to room temperature, and subsequently filtered over celite (eluted with EtOAc). Volatiles were removed under vacuum. The product was purified using silica column chromatography [eluted with CyH/(EtOAc:EtOH 3:1), gradient 100:0 to 0:100]. The fractions containing the product were further purified by reverse phase

chromatography (eluent MeCN/ H<sub>2</sub>O, gradient 0:100 to 100:0) to give 4-oxo-19-OH-carlactone as a colorless film (4.0 mg) that could be stored at −18°C in solution in DCM (4 mL).

#### SL extraction, LC-MS analysis, and LC-MS data processing

Rice seeds were pregerminated on moistened filter paper in a petri dish, and then four to five seedlings were transferred into 1-liter plastic pots with moistened river sand (0.5 to 1 mm) and watered with half-strength Hoagland solution (79). The seedlings were grown in a greenhouse chamber at 12 hours 30°C:12 hours 28°C photoperiod (supplemented by artificial light of 600 W/m<sup>2</sup> under low natural light conditions). After 3 weeks, Pi starvation was applied to induce SL production (13, 21, 80). After Pi deprivation of 1 week, 300 ml of root exudate from each pot was collected. The extraction of SLs from root exudate, *N. benthamiana* leaf, and yeast microsome assays was performed as previously described (28). The qualitative and quantitative analysis of SLs were performed as previously described (19, 28, 31, 81).

#### Gene cloning and transient expression in *N. benthamiana*

After extraction of total RNA from Nipponbare seedling roots, cDNA was synthesized using RevertAid H Minus Reverse Transcriptase (Thermo Fisher Scientific). The primers used for cloning full sequences of rice genes (*Os4OCLAMT1*, *Os4OCLAMT2*, and *OsCYP706C2*) are listed in table S3. Gas chromatography (GC) buffer and Phusion polymerase (Thermo Fisher Scientific) were used in PCR amplification (as sequences of rice genes are normally GC rich and decreasing PCR efficiency). Agroinfiltration was done following the method previously described by Li *et al.* (28).

#### In vitro assay using yeast microsomes

WT yeast strain WAT11 was cultured using Yeast extract-Bactopectone-Glucose-Agar (YPGA) medium, while transformed yeast was sustained with SGI medium (19, 82). *OsCYP706C2* was cloned and ligated into pYeDP60 (table S2). Two plasmids (pYeDP60-*OsCYP706C2* and pYeDP60 empty vector) were transformed independently into WAT11 using the S. c. EasyComp Transformation Kit (Invitrogen). Induction of gene expression in yeast and yeast microsome extraction were done following published protocols (19, 28, 82). Microsome assays were performed in an enzyme-free 2-ml Eppendorf tube containing substrate (MeCLA, 5 µl from 200 µM stock in dimethyl sulfoxide), 1 mM reduced form of nicotinamide adenine dinucleotide phosphate, 40 mM phosphate buffer, 100 µl of microsomal protein (*OsCYP706C2*), and autoclaved Milli-Q water (to complement the total amount of 500 µl).

#### *S. hermonthica* germination bioassay

*S. hermonthica* (*Striga*) seeds were sterilized in a solution containing 2% bleach and 0.02% Tween 20. After 5-min shaking and removal of the solution, the seeds were further cleaned with autoclaved Milli-Q water (five times). Seeds were preconditioned on the surface of filter paper in a petri dish at 30°C in the dark. After 11 days, germination bioassays were carried out using diluted root exudate samples, GR24 and SL standards, in a well in a 12-well plate, with three biological and three technical replicates.

#### Mycorrhizal colonization assays

WT cv. Nipponbare and three mutant lines of *oscyp706c2* were grown and assessed for *Rhizophagus irregularis* DAOM 197198 colonization as described before (83, 84). Plants were sampled 14- and 50-dpi,

corresponding to the early and late stages of mycorrhization (83, 84). Staining of the roots, assessment of colonization rate, and arbuscule phenotype were done as previously described (85). Quantitative reverse transcription PCR assays of the two AM-responsive marker genes *OsPT11* and *OsLysM* were performed according to Chen *et al.* (49).

#### Statistics

Unless noted otherwise, data are the means ± SE of *n* replicates, and *P* values were calculated using one-way analysis of variance (ANOVA).

#### Supplementary Materials

This PDF file includes:

Figs. S1 to S13

Legends for tables S1 to S8

Other Supplementary Material for this manuscript includes the following:

Tables S1 to S8

#### REFERENCES AND NOTES

- Gomez-Roldan, S. Fernas, P. B. Brewer, V. Puech-Pagès, E. A. Dun, J.-P. Pillot, F. Letisse, R. Matusova, S. Danoun, J.-C. Portais, H. Bouwmeester, G. Bécard, C. A. Beveridge, C. Rameau, S. F. Rochange, Strigolactone inhibition of shoot branching. *Nature* **455**, 189–194 (2008).
- Umehara, A. Hanada, S. Yoshida, K. Akiyama, T. Arite, N. Takeda-Kamiya, H. Magome, Y. Kamiya, K. Shirasu, K. Yoneyama, J. Kyojuka, S. Yamaguchi, Inhibition of shoot branching by new terpenoid plant hormones. *Nature* **455**, 195–200 (2008).
- K. C. Snowden, A. J. Simkin, B. J. Janssen, K. R. Templeton, H. M. Loucas, J. L. Simons, S. Karunairatnam, A. P. Gleave, D. G. Clark, H. J. Klee, *The Decreased apical dominance1/Petunia hybrida* CAROTENOID CLEAVAGE DIOXYGENASE8 gene affects branch production and plays a role in leaf senescence, root growth, and flower development. *Plant Cell* **17**, 746–759 (2005).
- C. Ruyter-Spira, W. Kohlen, T. Charnikhova, A. van Zeijl, L. van Bezouwen, N. de Ruijter, C. Cardoso, J. A. Lopez-Raez, R. Matusova, R. Bours, F. Verstappen, H. Bouwmeester, Physiological effects of the synthetic strigolactone analog GR24 on root system architecture in *Arabidopsis*: Another belowground role for strigolactones? *Plant Physiol.* **155**, 721–734 (2011).
- K. Yoneyama, A. A. Awad, X. Xie, K. Yoneyama, Y. Takeuchi, Strigolactones as germination stimulants for root parasitic plants. *Plant Cell Physiol.* **51**, 1095–1103 (2010).
- S. Al-Babili, H. J. Bouwmeester, Strigolactones, a novel carotenoid-derived plant hormone. *Annu. Rev. Plant Biol.* **66**, 161–186 (2015).
- H. Bouwmeester, C. Li, B. Thiombiano, M. Rahimi, L. Dong, Adaptation of the parasitic plant lifecycle: Germination is controlled by essential host signaling molecules. *Plant Physiol.* **185**, 1292–1308 (2021).
- J. Clark, T. Bennett, Cracking the enigma: Understanding strigolactone signalling in the rhizosphere. *J. Exp. Bot.* **75**, 1159–1173 (2024).
- X. Xie, K. Yoneyama, T. Kisugi, K. Uchida, S. Ito, K. Akiyama, H. Hayashi, T. Yokota, T. Nomura, K. Yoneyama, Confirming stereochemical structures of strigolactones produced by rice and tobacco. *Mol. Plant* **6**, 153–163 (2013).
- H. I. Kim, T. Kisugi, P. Khetkam, X. Xie, K. Yoneyama, K. Uchida, T. Yokota, T. Nomura, C. S. McElean, K. Yoneyama, Avenaol, a germination stimulant for root parasitic plants from *Avena strigosa*. *Phytochemistry* **103**, 85–88 (2014).
- K. Ueno, T. Furumoto, S. Umeda, M. Mizutani, H. Takikawa, R. Batchvarova, Y. Sugimoto, Helioactone, a non-sesquiterpene lactone germination stimulant for root parasitic weeds from sunflower. *Phytochemistry* **108**, 122–128 (2014).
- Y. Seto, A. Sado, K. Asami, A. Hanada, M. Umehara, K. Akiyama, S. Yamaguchi, Carlactone is an endogenous biosynthetic precursor for strigolactones. *Proc. Natl. Acad. Sci. U.S.A.* **111**, 1640–1645 (2014).
- T. V. Charnikhova, K. Gaus, A. Lumbroso, M. Sanders, J.-P. Vincken, A. De Mesmaeker, C. P. Ruyter-Spira, C. Screpanti, H. J. Bouwmeester, Zealactones. Novel natural strigolactones from maize. *Phytochemistry* **137**, 123–131 (2017).
- T. V. Charnikhova, K. Gaus, A. Lumbroso, M. Sanders, J.-P. Vincken, A. De Mesmaeker, C. P. Ruyter-Spira, C. Screpanti, H. J. Bouwmeester, Zeapyranolactone—A novel strigolactone from maize. *Phytochem. Lett.* **24**, 172–178 (2018).



15. K. Yoneyama, X. Xie, K. Yoneyama, T. Kisugi, T. Nomura, Y. Nakatani, K. Akiyama, C. S. McElean, Which are the major players, canonical or non-canonical strigolactones? *J. Exp. Bot.* **69**, 2231–2239 (2018).
16. R. Matusova, K. Rani, F. W. Verstappen, M. C. Franssen, M. H. Beale, H. J. Bouwmeester, The strigolactone germination stimulants of the plant-parasitic *Striga* and *Orobancha* spp. are derived from the carotenoid pathway. *Plant Physiol.* **139**, 920–934 (2005).
17. A. Alder, M. Jamil, M. Marzorati, M. Bruno, M. Vermathen, P. Bigler, S. Ghisla, H. Bouwmeester, P. Beyer, S. Al-Babili, The path from  $\beta$ -carotene to carlactone, a strigolactone-like plant hormone. *Science* **335**, 1348–1351 (2012).
18. S. Abe, A. Sado, K. Tanaka, T. Kisugi, K. Asami, S. Ota, H. I. Kim, K. Yoneyama, X. Xie, T. Ohnishi, Carlactone is converted to carlactonoic acid by MAX1 in Arabidopsis and its methyl ester can directly interact with AtD14 in vitro. *Proc. Natl. Acad. Sci. U.S.A.* **111**, 18084–18089 (2014).
19. Y. Zhang, A. D. Van Dijk, A. Scaffidi, G. R. Flematti, M. Hofmann, T. Charnikhova, F. Verstappen, J. Hepworth, S. Van Der Krol, O. Leyser, Rice cytochrome P450 MAX1 homologs catalyze distinct steps in strigolactone biosynthesis. *Nat. Chem. Biol.* **10**, 1028–1033 (2014).
20. K. Yoneyama, N. Mori, T. Sato, A. Yoda, X. Xie, M. Okamoto, M. Iwanaga, T. Ohnishi, H. Nishiwaki, T. Asami, Conversion of carlactone to carlactonoic acid is a conserved function of MAX1 homologs in strigolactone biosynthesis. *New Phytol.* **218**, 1522–1533 (2018).
21. Y. Zhang, X. Cheng, Y. Wang, C. Díez-Simón, K. Flokova, A. Bimbo, H. J. Bouwmeester, C. Ruyter-Spira, The tomato MAX1 homolog, SIMAX1, is involved in the biosynthesis of tomato strigolactones from carlactone. *New Phytol.* **219**, 297–309 (2018).
22. K. Mashiguchi, Y. Seto, Y. Onozuka, S. Suzuki, K. Takemoto, Y. Wang, L. Dong, K. Asami, R. Noda, T. Kisugi, A carlactonoic acid methyltransferase that contributes to the inhibition of shoot branching in Arabidopsis. *Proc. Natl. Acad. Sci. U.S.A.* **119**, e2111565119 (2022).
23. T. Wakabayashi, K. Shida, Y. Kitano, H. Takikawa, M. Mizutani, Y. Sugimoto, CYP722C from *Gossypium arboreum* catalyzes the conversion of carlactonoic acid to 5-deoxystrigol. *Planta* **251**, 97 (2020).
24. N. Mori, T. Nomura, K. Akiyama, Identification of two oxygenase genes involved in the respective biosynthetic pathways of canonical and non-canonical strigolactones in *Lotus japonicus*. *Planta* **251**, 40 (2020).
25. T. Wakabayashi, M. Hamana, A. Mori, R. Akiyama, K. Ueno, K. Osakabe, Y. Osakabe, H. Suzuki, H. Takikawa, M. Mizutani, Direct conversion of carlactonoic acid to orobanchol by cytochrome P450 CYP722C in strigolactone biosynthesis. *Sci. Adv.* **5**, eaax9067 (2019).
26. T. Wakabayashi, S. Ishiwa, K. Shida, N. Motonami, H. Suzuki, H. Takikawa, M. Mizutani, Y. Sugimoto, Identification and characterization of sorgomol synthase in sorghum strigolactone biosynthesis. *Plant Physiol.* **185**, 902–913 (2021).
27. Y. Wang, J. Durairaj, H. G. Suárez Duran, R. van Velzen, K. Flokova, C. Y. Liao, A. Chojnacka, S. MacFarlane, M. E. Schranz, M. H. Medema, A. D. J. van Dijk, L. Dong, H. J. Bouwmeester, The tomato cytochrome P450 CYP712G1 catalyses the double oxidation of orobanchol en route to the rhizosphere signalling strigolactone, solanacol. *New Phytol.* **235**, 1884–1899 (2022).
28. C. Li, L. Dong, J. Durairaj, J.-C. Guan, M. Yoshimura, P. Quinodoz, R. Horber, K. Gaus, J. Li, Y. Setotaw, Maize resistance to witchweed through changes in strigolactone biosynthesis. *Science* **379**, 94–99 (2023).
29. M. Jamil, J. Rodenburg, T. Charnikhova, H. J. Bouwmeester, Pre-attachment *Striga* hermonthica resistance of New Rice for Africa (NERICA) cultivars based on low strigolactone production. *New Phytol.* **192**, 964–975 (2011).
30. M. Jamil, T. Charnikhova, B. Houshyani, A. van Ast, H. J. Bouwmeester, Genetic variation in strigolactone production and tillering in rice and its effect on *Striga hermonthica* infection. *Planta* **235**, 473–484 (2012).
31. C. Cardoso, Y. Zhang, M. Jamil, J. Hepworth, T. Charnikhova, S. O. Dimkpa, C. Meharg, M. H. Wright, J. Liu, X. Meng, Natural variation of rice strigolactone biosynthesis is associated with the deletion of two MAX1 orthologs. *Proc. Natl. Acad. Sci. U.S.A.* **111**, 2379–2384 (2014).
32. Y. Wang, H. G. S. Duran, J. C. van Haarst, E. G. Schijlen, C. Ruyter-Spira, M. H. Medema, L. Dong, H. J. Bouwmeester, The role of strigolactones in P deficiency induced transcriptional changes in tomato roots. *BMC Plant Biol.* **21**, 1–21 (2021).
33. I. Haider, Z. Yunmeng, F. White, C. Li, R. Incitti, I. Alam, T. Gojobori, C. Ruyter-Spira, S. Al-Babili, H. J. Bouwmeester, Transcriptome analysis of the phosphate starvation response sheds light on strigolactone biosynthesis in rice. *Plant J.* **114**, 355–370 (2023).
34. T.-Y. Liu, T.-K. Huang, S.-Y. Yang, Y.-T. Hong, S.-M. Huang, F.-N. Wang, S.-F. Chiang, S.-Y. Tsai, W.-C. Lu, T.-J. Chiou, Identification of plant vacuolar transporters mediating phosphate storage. *Nat. Commun.* **7**, 11095 (2016).
35. M. Rebers, T. Kaneta, H. Kawaide, S. Yamaguchi, Y. Y. Yang, R. Imai, H. Sekimoto, Y. Kamiya, Regulation of gibberellin biosynthesis genes during flower and early fruit development of tomato. *Plant J.* **17**, 241–250 (1999).
36. K. Otomo, H. Kenmoku, H. Oikawa, W. A. König, H. Toshiwa, W. Mitsuhashi, H. Yamane, T. Sassa, T. Toyomasu, Biological functions of *ent*- and *syn*-copalyl diphosphate synthases in rice: Key enzymes for the branch point of gibberellin and phytoalexin biosynthesis. *Plant J.* **39**, 886–893 (2004).
37. J. Li, W. Sima, B. Ouyang, T. Wang, K. Ziaf, Z. Luo, L. Liu, H. Li, M. Chen, Y. Huang, Y. Feng, Y. Hao, Z. Ye, Tomato *SIDREB* gene restricts leaf expansion and internode elongation by downregulating key genes for gibberellin biosynthesis. *J. Exp. Bot.* **63**, 6407–6420 (2012).
38. H. Itoh, T. Tatsumi, T. Sakamoto, K. Otomo, T. Toyomasu, H. Kitano, M. Ashikari, S. Ichihara, M. Matsuoka, A rice semi-dwarf gene, *Tan-Ginbozo (D35)*, encodes the gibberellin biosynthesis enzyme, *ent*-kaurene oxidase. *Plant Mol. Biol.* **54**, 533–547 (2004).
39. F. Barbier, F. Fichtner, C. Beveridge, The strigolactone pathway plays a crucial role in integrating metabolic and nutritional signals in plants. *Nat. Plants* **9**, 1191–1200 (2023).
40. K. Akiyama, K.-i. Matsuzaki, H. Hayashi, Plant sesquiterpenes induce hyphal branching in arbuscular mycorrhizal fungi. *Nature* **435**, 824–827 (2005).
41. K. Kodama, M. K. Rich, A. Yoda, S. Shimazaki, X. Xie, K. Akiyama, Y. Mizuno, A. Komatsu, Y. Luo, H. Suzuki, H. Kameoka, C. Libourel, J. Keller, K. Sakakibara, T. Nishiyama, T. Nakagawa, K. Mashiguchi, K. Uchida, K. Yoneyama, Y. Tanaka, S. Yamaguchi, M. Shimamura, P. M. Delaux, T. Nomura, J. Kyojuka, An ancestral function of strigolactones as symbiotic rhizosphere signals. *Nat. Commun.* **13**, 3974 (2022).
42. D. Secco, M. Jabnour, H. Walker, H. Shou, P. Wu, Y. Poirier, J. Whelan, Spatio-temporal transcript profiling of rice roots and shoots in response to phosphate starvation and recovery. *Plant Cell* **25**, 4285–4304 (2013).
43. E. Poretsky, A. Huffaker, MutRank: An R shiny web-application for exploratory targeted mutual rank-based coexpression analyses integrated with user-provided supporting information. *PeerJ* **8**, e10264 (2020).
44. Y. Li, K. Wei, Comparative functional genomics analysis of cytochrome P450 gene superfamily in wheat and maize. *BMC Plant Biol.* **20**, 1–22 (2020).
45. T. Wakabayashi, R. Yasuhara, K. Miura, H. Takikawa, M. Mizutani, Y. Sugimoto, Specific methylation of (11R)-carlactonoic acid by an Arabidopsis SABATH methyltransferase. *Planta* **254**, 88 (2021).
46. L. Xia, D. Zou, J. Sang, X. Xu, H. Yin, M. Li, S. Wu, S. Hu, L. Hao, Z. Zhang, Rice Expression Database (RED): An integrated RNA-Seq-derived gene expression database for rice. *J. Genet. Genomics* **44**, 235–241 (2017).
47. M. C. Dieckmann, P.-Y. Dakas, A. De Mesmaeker, Synthetic access to noncanonical strigolactones: Syntheses of carlactonic acid and methyl carlactonoate. *J. Org. Chem.* **83**, 125–135 (2018).
48. S. Ito, J. Braguy, J. Y. Wang, A. Yoda, V. Fiorilli, I. Takahashi, M. Jamil, A. Felemban, S. Miyazaki, T. Mazzarella, G. E. Chen, A. Shinozawa, A. Balakrishna, L. Berqdar, C. Rajan, S. Ali, I. Haider, Y. Sasaki, S. Yajima, K. Akiyama, L. Lanfranco, M. D. Zurbruggen, T. Nomura, T. Asami, S. Al-Babili, Canonical strigolactones are not the major determinant of tillering but important rhizospheric signals in rice. *Sci. Adv.* **8**, eadd1278 (2022).
49. G.-T. E. Chen, J. Y. Wang, C. Votta, J. Braguy, M. Jamil, G. K. Kirschner, V. Fiorilli, L. Berqdar, A. Balakrishna, I. Blilou, L. Lanfranco, S. Al-Babili, Disruption of the rice4-DEOXYOROBANCHOL HYDROXYLASE unravels specific functions of canonical strigolactones. *Proc. Natl. Acad. Sci. U.S.A.* **120**, e2306263120 (2023).
50. U. Paszkowski, S. Kroken, C. Roux, S. P. Briggs, Rice phosphate transporters include an evolutionarily divergent gene specifically activated in arbuscular mycorrhizal symbiosis. *Proc. Natl. Acad. Sci. U.S.A.* **99**, 13324–13329 (2002).
51. V. Fiorilli, M. Vallino, C. Biselli, A. Faccio, P. Bagnaresi, P. Bonfante, Host and non-host roots in rice: Cellular and molecular approaches reveal differential responses to arbuscular mycorrhizal fungi. *Front. Plant Sci.* **6**, 636 (2015).
52. K. Mashiguchi, Y. Seto, S. Yamaguchi, Strigolactone biosynthesis, transport and perception. *Plant J.* **105**, 335–350 (2020).
53. X. Xie, T. Kisugi, K. Yoneyama, T. Nomura, K. Akiyama, K. Uchida, T. Yokota, C. S. McElean, K. Yoneyama, Methyl zealactonoate, a novel germination stimulant for root parasitic weeds produced by maize. *J. Pestic. Sci.* **42**, 58–61 (2017).
54. N. Mori, K. Nishiuma, T. Sugiyama, H. Hayashi, K. Akiyama, Carlactone-type strigolactones and their synthetic analogues as inducers of hyphal branching in arbuscular mycorrhizal fungi. *Phytochemistry* **130**, 90–98 (2016).
55. X. Xie, N. Mori, K. Yoneyama, T. Nomura, K. Uchida, K. Yoneyama, K. Akiyama, Lotuslactone, a non-canonical strigolactone from *Lotus japonicus*. *Phytochemistry* **157**, 200–205 (2019).
56. K. Ueno, S. Nomura, S. Muranaka, M. Mizutani, H. Takikawa, Y. Sugimoto, *Ent*-2'-*epi*-orobanchol and its acetate, as germination stimulants for *Striga gesnerioides* seeds isolated from cowpea and red clover. *J. Agric. Food Chem.* **59**, 10485–10490 (2011).
57. S. Nomura, H. Nakashima, M. Mizutani, H. Takikawa, Y. Sugimoto, Structural requirements of strigolactones for germination induction and inhibition of *Striga gesnerioides* seeds. *Plant Cell Rep.* **32**, 829–838 (2013).
58. J. Cui, N. Nishide, K. Mashiguchi, K. Kuroha, M. Miya, K. Sugimoto, J.-I. Itoh, S. Yamaguchi, T. Izawa, Fertilization controls tiller numbers via transcriptional regulation of a MAX1-like gene in rice cultivation. *Nat. Commun.* **14**, 3191 (2023).
59. J. C. Guan, K. E. Koch, M. Suzuki, S. Wu, S. Latshaw, T. Petrucci, C. Goulet, H. J. Klee, D. R. McCarty, Diverse roles of strigolactone signaling in maize architecture and the uncoupling of a branching-specific subnetwork. *Plant Physiol.* **160**, 1303–1317 (2012).



60. Y. An, Y. Ma, J. Shui, W. Zhong, Switchgrass (*Panicum virgatum*L.) has ability to induce germination of *Orobanche cumana*. *J. Plant Interact.* **10**, 142–151 (2015).
61. J. Chen, Q. Huang, D. Gao, J. Wang, Y. Lang, T. Liu, B. Li, Z. Bai, J. L. Goicoechea, C. Liang, C. Chen, W. Zhang, S. Sun, Y. Liao, X. Zhang, L. Yang, C. Song, M. Wang, J. Shi, G. Liu, J. Liu, H. Zhou, W. Zhou, Q. Yu, N. An, Y. Chen, Q. Cai, B. Wang, B. Liu, J. Min, Y. Huang, H. Wu, Z. Li, Y. Zhang, Y. Yin, W. Song, J. Jiang, S. A. Jackson, R. A. Wing, J. Wang, M. Chen, Whole-genome sequencing of *Oryza brachyantha* reveals mechanisms underlying *Oryza* genome evolution. *Nat. Commun.* **4**, 1595 (2013).
62. B. Kim, J. A. Westerhuis, A. K. Smilde, K. Floková, A. K. A. Suleiman, E. E. Kuramae, H. J. Bouwmeester, A. Zancanini, Effect of strigolactones on recruitment of the rice root-associated microbiome. *FEMS Microbiol. Ecol.* **98**, fiac010 (2022).
63. M. Robinson, D. J. McCarthy, G. K. Smyth, edgeR: A bioconductor package for differential expression analysis of digital gene expression data. *Biogeosciences* **26**, 139–140 (2010).
64. D. R. Zerbinio, P. Achuthan, W. Akanni, M. R. Amode, D. Barrell, J. Bhai, K. Billis, C. Cummins, A. Gall, C. G. Girón, L. Gil, L. Gordon, L. Haggerty, E. Haskell, T. Hourlier, O. G. Izuogu, S. H. Janacek, T. Juettemann, M. R. Laird, I. Lavidas, Z. Liu, J. E. Loveland, T. Maurel, W. McLaren, B. Moore, J. Mudge, D. N. Murphy, V. Newman, M. Nuhn, D. Ogeh, C. K. Ong, A. Parker, M. Patricio, H. S. Riat, H. Schuilenburg, D. Sheppard, H. Sparrow, K. Taylor, A. Thormann, A. Vullo, B. Walts, A. Zadissa, A. Frankish, S. E. Hunt, M. Kostadima, N. Langridge, F. J. Martin, M. Muffato, E. Perry, M. Ruffier, D. M. Staines, S. J. Trevanion, B. L. Aken, F. Cunningham, A. Yates, P. Flicek, Ensembl 2018. *Nucleic Acids Res.* **46**, D754–D761 (2018).
65. D. Smedley, S. Haider, B. Ballester, R. Holland, D. London, G. Thorisson, A. Kasprzyk, BioMart—Biological queries made easy. *BMC Genomics* **10**, 22 (2009).
66. R. Team, “RStudio: Integrated development for R” (RStudio, PBC, 2020).
67. C. L. Gilchrist, T. J. Booth, B. van Wersch, L. van Grieken, M. H. Medema, Y.-H. Chooi, cblaster: A remote search tool for rapid identification and visualization of homologous gene clusters. *Bioinform. Adv.* **1**, vbab016 (2021).
68. R. D. Finn, P. Coghill, R. Y. Eberhardt, S. R. Eddy, J. Mistry, A. L. Mitchell, S. C. Potter, M. Punta, M. Qureshi, A. Sangrador-Vegas, The Pfam protein families database: Towards a more sustainable future. *Nucleic Acids Res.* **44**, D279–D285 (2016).
69. J. Mistry, R. D. Finn, S. R. Eddy, A. Bateman, M. Punta, Challenges in homology search: HMMER3 and convergent evolution of coiled-coil regions. *Nucleic Acids Res.* **41**, e121–e121 (2013).
70. C. Camacho, G. Coulouris, V. Avagyan, N. Ma, J. Papadopoulos, K. Bealer, T. L. Madden, BLAST+: Architecture and applications. *BMC Bioinformatics* **10**, 421 (2009).
71. C. Notredame, D. G. Higgins, J. Heringa, T-Coffee: A novel method for fast and accurate multiple sequence alignment. *J. Mol. Biol.* **302**, 205–217 (2000).
72. D. R. Nelson, The cytochrome p450 homepage. *Hum. Genomics* **4**, 59 (2009).
73. S. Capella-Gutiérrez, J. M. Silla-Martínez, T. Gabaldón, trimAl: A tool for automated alignment trimming in large-scale phylogenetic analyses. *Bioinformatics* **25**, 1972–1973 (2009).
74. A. Stamatakis, RAxML version 8: A tool for phylogenetic analysis and post-analysis of large phylogenies. *Bioinformatics* **30**, 1312–1313 (2014).
75. K. Xie, B. Minkenberg, Y. Yang, Boosting CRISPR/Cas9 multiplex editing capability with the endogenous tRNA-processing system. *Proc. Natl. Acad. Sci. U.S.A.* **112**, 3570–3575 (2015).
76. Y. Hiei, T. Komari, *Agrobacterium*-mediated transformation of rice using immature embryos or calli induced from mature seed. *Nat. Protoc.* **3**, 824–834 (2008).
77. M. Yoshimura, R. Fonné-Pfister, C. Screpanti, K. Hermann, S. Rendine, M. Dieckmann, P. Quinodoz, A. De Mesmaeker, Total synthesis and biological evaluation of heliolactone. *Helv. Chim. Acta* **102**, e1900211 (2019).
78. M. Domínguez, S. Álvarez, R. Álvarez, Á. R. de Lera, Stereocontrolled synthesis of (S)-9-cis-4-oxo-13, 14-dihydroretinoic acid. *Tetrahedron* **68**, 1756–1761 (2012).
79. N. Mohamed, T. Charnikhova, E. J. Bakker, A. van Ast, A. G. Babiker, H. J. Bouwmeester, Evaluation of field resistance to *Striga hermonthica* (Del.) Benth. in *Sorghum bicolor* (L.) Moench. The relationship with strigolactones. *Pest Manag. Sci.* **72**, 2082–2090 (2016).
80. J. A. López-Ráez, T. Charnikhova, V. Gómez-Roldán, R. Matusova, W. Kohlen, R. De Vos, F. Verstappen, V. Puech-Pages, G. Bécard, P. Mulder, Tomato strigolactones are derived from carotenoids and their biosynthesis is promoted by phosphate starvation. *New Phytol.* **178**, 863–874 (2008).
81. J. Y. Wang, G.-T. E. Chen, M. Jamil, J. Braguy, S. Sioud, K. X. Liew, A. Balakrishna, S. Al-Babili, Protocol for characterizing strigolactones released by plant roots. *STAR Protocols* **3**, 101352 (2022).
82. D. Pompon, B. Louerat, A. Bronine, P. Urban, Yeast expression of animal and plant P450s in optimized redox environments. *Methods Enzymol.* **272**, 51–64 (1996).
83. C. Votta, V. Fiorilli, I. Haider, J. Y. Wang, R. Balestrini, I. Petřík, D. Tarkovská, O. Novák, A. Serikbayeva, P. Bonfante, Zaxinone synthase controls arbuscular mycorrhizal colonization level in rice. *Plant J.* **111**, 1688–1700 (2022).
84. A. Ablazov, C. Votta, V. Fiorilli, J. Y. Wang, F. Aljedaani, M. Jamil, A. Balakrishna, R. Balestrini, K. X. Liew, C. Rajan, L. Berqdar, I. Bilou, L. Lanfranco, S. Al-Babili, ZAXINONE SYNTHASE 2 regulates growth and arbuscular mycorrhizal symbiosis in rice. *Plant Physiol.* **191**, 382–399 (2023).
85. A. Trouvelot, J. Kough, V. Gianinazzi-Pearson, Evaluation of VA infection levels in root systems. Research for estimation methods having a functional significance, in *Physiological and Genetical Aspects of Mycorrhizae*, V. Gianinazzi-Pearson, S. Gianinazzi, Eds. (INRA, 1986), pp. 217–221.

**Acknowledgments:** We would like to thank the staff from our collaborators' affiliations for the valuable contributions to this research. **Funding:** This work was supported by the China Scholarship Council (CSC) PhD scholarship 201706300041 (to C.L.); the China Ministry of Science and Technology High-end Foreign Experts Recruitment Plan G2023160023L (to C.L.); the Outstanding Youth Project of the Natural Science Foundation of Hunan Province 2024JJ2013 (to C.L.); the CAPES-Print Program 88887.570702/2020-00 (S.M.C.d.L.); the Agritech National Research Center, the European Union Next-Generation EU (PIANO NAZIONALE DI RIPRESA E RESILIENZA (PNRR) - MISSIONE 4 COMPONENTE 2, INVESTIMENTO 1.4 - D.D. 1032 17/06/2022) CN00000022 (to I.H.); the European Research Council (ERC) Advanced grant CHEMCOMRHIZO 670211 (to H.J.B.); the Dutch Research Council (NWO/OCW) Gravitation Programme Harnessing the second genome of plants (MiCRop) 024.004.014 (to H.J.B., L.D., and C.L.); the Marie Curie fellowship NEMHATCH 793795 (to L.D.); the Baseline funding from King Abdullah University of Science and Technology (KAUST) and the Bill & Melinda Gates Foundation (OPP1136424, SA); the National Biodiversity Future Center funded under the National Recovery and Resilience Plan (NRRP), Mission 4 Component 2 Investment 1.4 of the Italian Ministry of University CN00000033 (to V.F. and L.L.); the European Union–NextGenerationEU 2022CWZNCZ (to V.F. and L.L.); and the Netherlands Organization for Scientific Research (NWO) VENI Grant 863.15.002 (to M.H.M.). **Author contributions:** C.L., L.D., and H.J.B. designed the research. C.L., I.H., J.Y.W., P.Q., L.R.M., R.H., V.F., C.V., L.L., S.M.C.d.L., L.J., B.M., L.M., A.D.M., and S.A.-B. performed the research. C.L., I.H., L.R.M., V.F., C.V., L.L., H.G.S.D., S.M.C.d.L., M.H.M., S.A.-B., L.D., and H.J.B. analyzed the data. C.L., L.D., and H.J.B. wrote the manuscript. **Competing interests:** The authors declare that they have no competing interests. **Data and materials availability:** The rice *oscyp706c2* mutants can be provided by S.A.-B. pending scientific review and a completed material transfer agreement. Requests for the rice *oscyp706c2* mutants should be submitted to S.A.-B. All the other data needed to evaluate the conclusions in the paper are present in the paper and/or the Supplementary Materials.

Submitted 11 May 2024

Accepted 24 July 2024

Published 28 August 2024

10.1126/sciadv.adq3942